Acta geographica Slovenica, 66-1, 2026, 39–59

HIERARCHICAL CLUSTER CLASSIFICATION AND ANALYSIS OF CIRQUES IN SLOVENIAN ALPS

Klemen Cof, Uroš Stepišnik, Manja Žebre, Matej Lipar

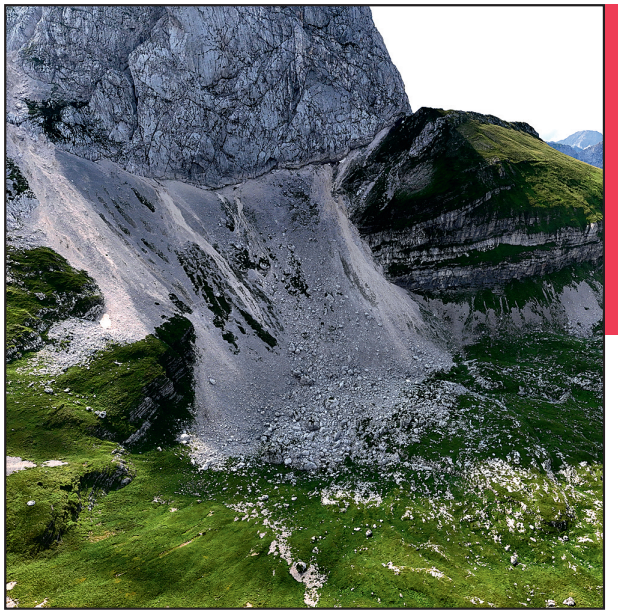

UROŠ STEPIŠNIK

The cirque under Mount Mangrt, Julian Alps.

DOI: https://doi.org/10.3986/AGS.14012
UDC: 551.435.42(497.4)(234.3)

Klemen Cof[1], Uroš Stepišnik[1], Manja Žebre[2], Matej Lipar[3]

Hierarchical cluster classification and analysis of cirques in Slovenian Alps

ABSTRACT: This paper presents a morphometry-based classification of cirques in Slovenia in the southeast European Alps. The classification was performed using a hierarchical cluster analysis and verified using ANOVA, Kruskal-Wallis, Watson's U^2 and Chi-square tests. 86 Slovenian cirques were categorized into five cirque types. Type 1, 2, 3 and 5 cirques indicate a formation by high-altitude (1800–2000 m) glaciers under varying conditions and on varied aspects (NNW, W, SE, E). Type 4 cirques indicate a formation by low-altitude (1500–1800 m) glaciers in areas of marginal glaciation on northeast aspects. This classification provides a rapid and consistent method of partitioning new cirque populations and offers a preliminary insight into the cirque population and palaeoclimate properties of Slovenia.

KEYWORDS: glacial geomorphology, cirques, hierarchical cluster analysis, analysis of variance, Slovenia, southeast European Alps

Hierarhično razvrščanje in analiza krnic v slovenskih Alpah

POVZETEK: V članku je predstavljena klasifikacija slovenskih krnic v jugovzhodnih evropskih Alpah na osnovi morfometričnih podatkov. Klasifikacija je bila izvedena s hierarhično metodo razvrščanja in nato preverjena z analizo variance ter testi Kruskal-Wallis, Watsonov U^2 in Hi-kvadrat. 86 slovenskih krnic je bilo razdeljenih v pet krniških tipov. Krniške tipe 1, 2, 3 in 5 so oblikovali ledeniki na visokih nadmorskih višinah (1800–2000 m) pod različnimi pogoji in na različnih ekspozicijah (SSZ, Z, JV, V). Krniški tip 4 so oblikovali ledeniki na nižjih nadmorskih višinah (1500–1800 m) na območjih robne poledenitve na severovzhodnih ekspozicijah. Klasifikacija nudi hitro in dosledno metodo deljenja novih krniških populacij in nudi prvi vpogled v krniško populacijo in paleopodnebne razmere v Sloveniji.

KLJUČNE BESEDE: glacialna geomorfologija, krnice, hierarhična metoda razvrščanja, analiza variance, Slovenija, jugovzhodne evropske Alpe

The article was submitted for publication on November 28th, 2024.
Uredništvo je prejelo prispevek 28. novembra 2024.

[1] University of Ljubljana, Faculty of Arts, Ljubljana, Slovenia
[2] Geological Survey of Slovenia, Ljubljana, Slovenia
[3] Research Centre of the Slovenian Academy of Sciences and Arts, Ljubljana, Slovenia

cof.nagrand@gmail.com (https://orcid.org/0009–0003–7478–6050), uros.stepisnik@gmail.com (https://orcid.org/0000–0002–8475–8630), manja.zebre@geo–zs.si (https://orcid.org/0000–0001–6772–2866), matej.lipar@zrc–sazu.si (https://orcid.org/0000–0003–4414–0147)

1 Introduction

Former mountain glaciers and their responses to past climate changes are valuable analogues for predicting how modern glacial environments may respond to future climate change (Knight and Harrison 2014). However, reconstructing former mountain glaciers to draw conclusions about past environmental conditions is a challenging task, especially when the glacial source area relationship is not straightforward (Carr and Coleman 2007). Cirques, however, tend to have a very well-defined glacial area and have often been used as palaeoenvironmental proxies based on their morphology and morphometry, particularly in remote and inaccessible regions where other proxies may be limited or non-existent (e.g., Evans 2006b; Barr and Spagnolo 2013; Barr and Spagnolo 2015; Barr et al. 2017).

Cirques are concave hollows formed by glacial erosion with gently sloping floors bounded upstream by an arcuate steep headwall. Downstream they often have a reverse slope called a cirque threshold (Barr and Spagnolo 2015). The cirque floor is often overdeepened under the altitude of the cirque threshold (Evans 1997). Cirques typically form beneath mountain ridges at elevated altitudes (Evans 2006a), preferring shaded poleward aspects unless other factors (e.g., precipitation, bedrock, winds, weathering and chemical denudation) compensate for increased ablation due to exposure to solar radiation (Evans and McClean 1995; Coleman et al. 2009; Barr et al. 2017; Steinemann et al. 2020). It is specified that for a feature to be classified as a cirque, it should have headwall slopes exceeding 35° and floor slopes less than 20° in at least some sections (Evans and Cox 1974).

Cirques form mainly during the early and late stages of glaciation when glaciers are confined to their cirques (Barr and Spagnolo 2015) and when the equilibrium lines are located at the altitudes of cirque floors, leading to maximized subglacial erosion and the development of overdeepened cirques (Mitchell and Montgomery 2006). During glacial maxima, equilibrium line altitudes (ELAs) fall below the altitude of cirque floors and the glacial ice within cirques either becomes frozen to its bed or flows down valley into glacial troughs – both cases mean a reduction in subglacial erosion and a shift towards shallower cirques (Barr and Spagnolo 2015; Dixon et al. 2016).

Classification partitions data into distinct subgroups according to shared characteristics (Gareth et al. 2013). Historically, the classification of cirques has been predominantly based either on morphological characteristics (e.g., Penck 1905; Vilborg 1984; Evans and Cox 1995) or key geomorphic processes (e.g., Evans and Cox 1974). However, these earlier classifications relied heavily on the subjective judgement of researchers to properly apply to new cirque populations. They required each new cirque to be examined in detail to determine its origin and underlying geomorphic processes before it could be classified, thus limiting the practicality of these classifications. A cirque classification based on morphometric variables would allow for rapid, objective, and automatic differentiation of entire cirque populations.

The aim of this paper is to create such a statistically verifiable cirque classification based on key morphometric cirque variables. Slovenia was used as the study area because its distinct cirque shapes indicate a good degree of segmentation in the population to test the classification on. At the same time, Slovenia's cirque population has yet to be systematically explored, which makes classification an essential first step in determining the existing cirque types and focusing field work into the most typical cirques of each type. It helps in determining the feasibility of various field analyses for individual cirque types and will allow for a systematic and thorough analysis of the factors that influenced the formation of Slovenia's cirque population.

2 Material and methods

2.1 Regional setting

Slovenia is located in a unique geographical position at the junction of the European Alps, the Pannonian Basin, the Dinaric Alps and the Mediterranean Sea (Perko et al. 2021), creating a diverse climate across its mountainous regions. The southwestern areas of Slovenia are influenced by a moderate Mediterranean climate, while the northwestern mountainous regions experience a mountain climate. This climate is marked by winter temperatures below –3°C and summer temperatures below or slightly above 10°C, depending on altitude (Komac et al. 2020; Ogrin et al. 2023). The mountainous region is composed mainly of limestones

and dolomites which are mostly a combination of Upper Triassic rocks of the Julian Carbonate Platform to the north and Mesozoic rocks of the Slovenian Basin to the south. The eastern parts of the Karawanks are partially comprised of Palaeozoic limestones, sandstones, and flysch shales. Many valleys and basins are covered by Quaternary carbonate deposits of glacial, fluvial and colluvial origin. The Periadriatic fault crosses the northeast part of the Kamnik-Savinja Alps while the Julian Alps are intersected by the Sava, Ravne and Idrija faults from north to south (Hrvatin et al. 2020).

Despite having relatively low altitudes compared to the other parts of the Alps, several mountainous regions of Slovenia (the Julian Alps, the Karawanks and the Kamnik-Savinja Alps) were glaciated during the last glacial maximum (LGM) (Figure 1). Large glaciers formed in the Soča and Sava valleys as well as the Bohinj basin in the Julian Alps. The reported ELAs using the toe-to-headwall altitude ratio method for these three glaciers were between 1090 m a.s.l. and 1280 m a.s.l. and the glaciers extended to altitudes as low as 500 m a.s.l. with a thickness of up to 700 m (Ferk et al. 2017; Hughes et al. 2021). Several smaller valleys in all three mountain ranges were glaciated while a smaller ice cap formed on the Kanin Plateau in the west. Cirques formed at higher altitudes of all three mountain ranges (Bavec 2001; Stojilković et al. 2013). The two Dinaric plateaus Snežnik in the south and Trnovski gozd in the west of Slovenia were also glaciated, and there is evidence of marginal glaciation in the Pohorje Hills in the northeast (Natek 2007; Žebre et al. 2013; Žebre and Stepišnik 2016; Kodelja et al. 2018). Due to a high intensity of postglacial erosion and denudation, many glaciogenic forms and sediments have been eroded or redeposited. Additionally, very few of the moraines have been dated. This makes the present knowledge of the LGM ice position in Slovenia inconclusive (Bavec and Verbič 2004; Hughes et al. 2021).

2.2 Detection of cirques

The process of cirque detection was conducted manually in the ESRI ArcGIS Pro software, using three data sources: high-resolution Lidar surface data (1 m × 1 m) from the Slovenian Environment Agency (2015),

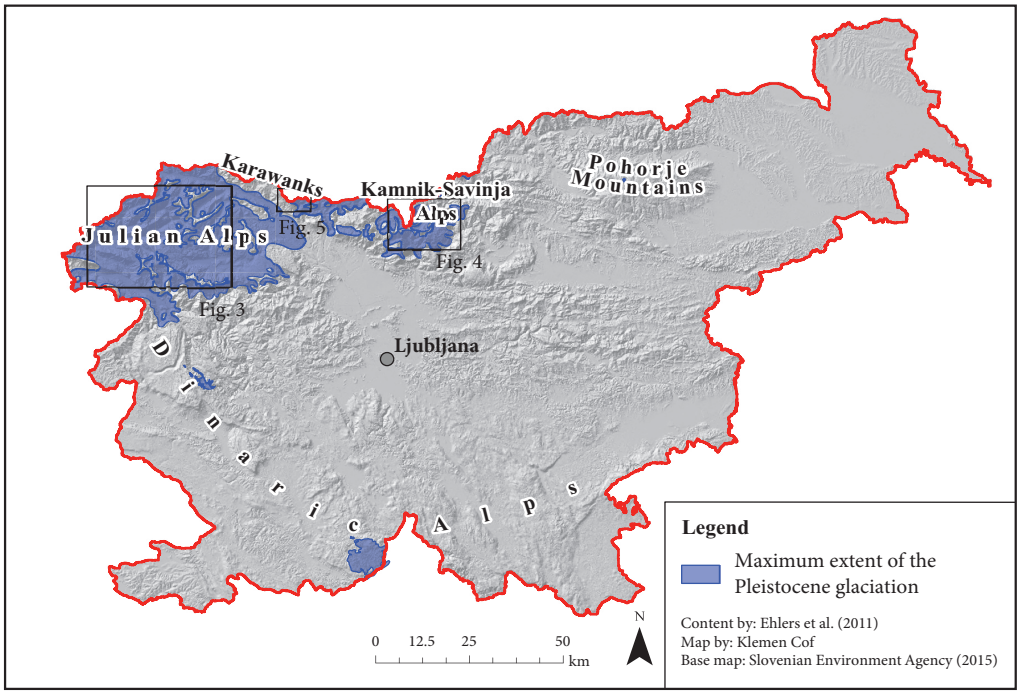

Figure 1: The maximum extent of the Pleistocene glaciation in Slovenia. Source of data: Ehlers et al. (2011); Slovenian Environment Agency (2015).

along with digital elevation models (DEMs) at resolutions of 5 m × 5 m and 12.5 m × 12.5 m provided by the Surveying and Mapping Authority of the Republic of Slovenia (2016a; 2016b). From the Lidar dataset, shaded relief was derived to enhance the visualization of topography, while the DEMs facilitated the extraction of slope and surface closure information (both plan and profile views). To mitigate data anomalies, the 5 m × 5 m DEM was smoothed using a 3 × 3 cell low pass filter. The 5 m × 5 m DEM was used over Lidar data for extracting slope data since the latter is too precise and more suited to small-scale analyses of individual cirques as opposed to broader analyses of cirque populations. Similarly, the 12.5 m × 12.5 m DEM was used for plan and profile closure extraction as the 5 m × 5 m data was too detailed to distinguish major ridges and gulleys. The following variables were used in the detection:

- Location: landforms at altitudes above 1100 m a.s.l. and relatively close to mountain ridges were considered, since cirques typically form only at the highest altitudes along mountain tops and ridges and since regional ELAs were reported at altitudes of 1090–1280 m a.s.l. (Ferk et al. 2017);
- Shape: in accordance with the definition, this research took into consideration concave landforms with a steep wall arcing around a flat floor that was open down-valley. Landforms with a height or diameter of less than 100 m were excluded as nivation hollows or niche glaciers (Evans and Cox 1974; Singh et al. 2011; Barr and Spagnolo 2015; Gutiérrez and Gutiérrez 2016);
- Slope: landforms with minimal floor slopes under 20° and maximal headwall slopes above 31–35° were considered. Gentler floor slopes are typical for cirques developed by a rotationally flowing glacier while headwall slopes steeper than talus slopes are indicative of more intense glacial erosion. Steeper headwall slopes separate cirques from nivation hollows. 26.6° was chosen as the slope threshold between headwalls and floors (Evans and Cox 1974; Evans 2006a; Barr and Spagnolo 2015);
- Plan and profile curvature: useful for accurate delineation of cirque extents. Where thresholds were absent, plan curvature was used to identify the spurs of the headwall to define the downward extent. Where profile closure did not show a clear upward extent, it was extended up to the cirque's overlying ridges. Landforms with a plan closure of less than 90° were excluded as nivation hollows (Hughes et al. 2007; Ardelean et al. 2013; Barr et al. 2017; Spagnolo et al. 2017).

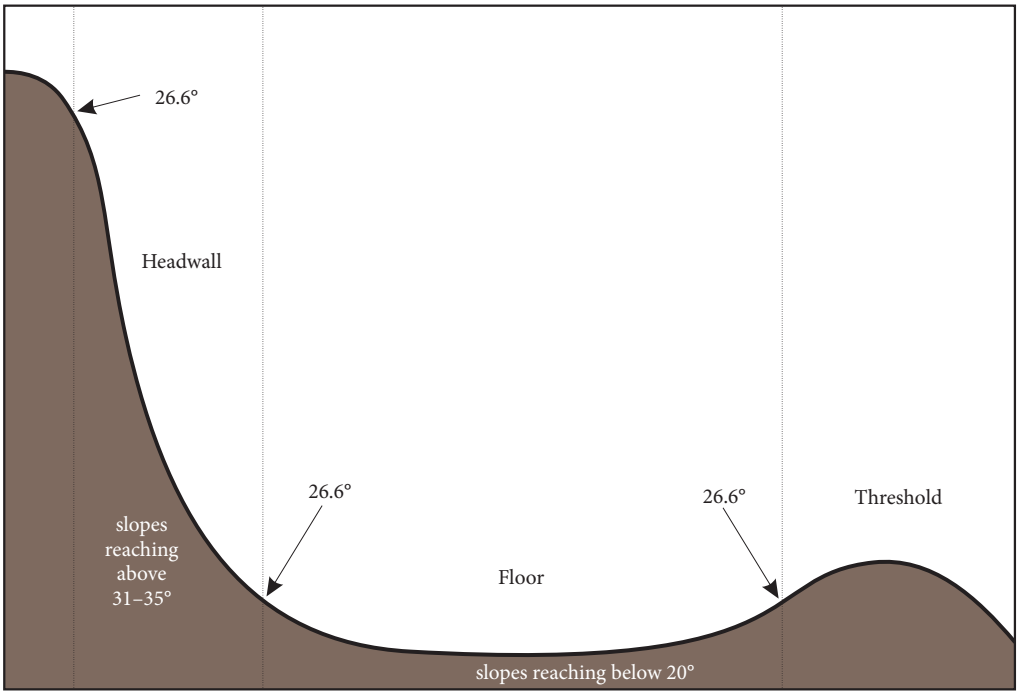

Figure 2: Schematic of a typical cirque's cross section.

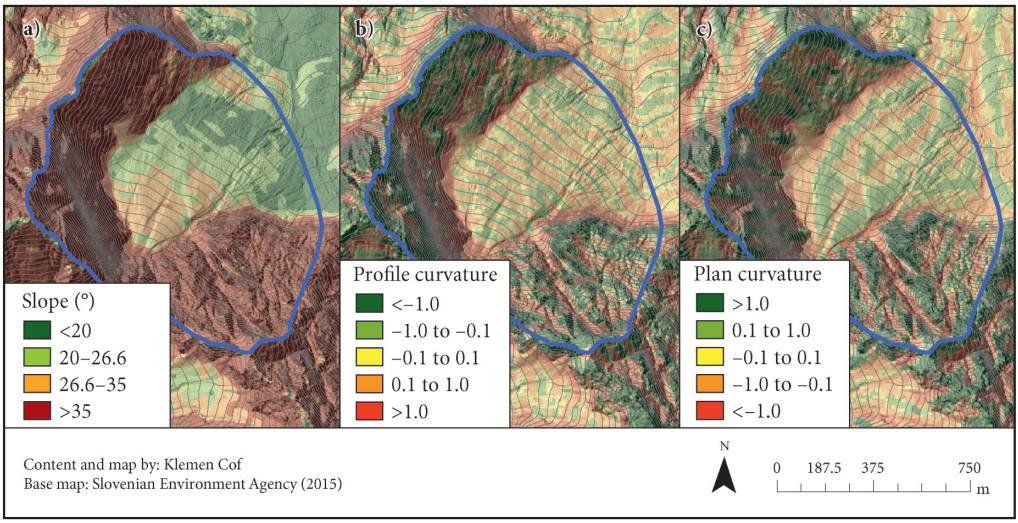

Figure 3: Example of cirque floor delineation. (A) Reclassified slope data and 20 m contours help delineate the cirque floor/headwall boundary. (B) Reclassified profile curvature data helps delineate the upward extent. (C) Reclassified plan curvature data helps delineate the spurs of the headwall.

Cirque delineation also involved separating the cirques into their respective cirque floors, headwalls, and thresholds based on their slopes (Figure 2) as well as the calculation of cirque threshold midpoints using the »Generate points along lines« function in ArcGIS. Figure 3 shows how various variables were used in the delineation of a sample cirque.

2.3 Morphometric analysis

For the analyses of the detected cirques, 14 morphometric variables were calculated, utilizing both manual techniques and the automated toolbox provided by Spagnolo et al. (2017). Table 1 shows the variables and their methods of calculation.

2.4 Classification

To classify the cirques a hierarchical cluster analysis was performed using the IBM SPSS Statistics 21 software, which was also used for many of the statistical analyses in the research. Hierarchical clustering does not require a predetermined number of clusters (Gareth et al. 2013), but is an exploratory method whose results require further validation (IBM 2021). Variables were standardized into Z scores to equalize the impact of variables with different value ranges (Zhenhua 2011).

Multiple sets of variables that cover key variables of cirques (see chapter 2.3) were entered into the analysis in a way that would enable the resulting classification to differentiate between cirques according to those variables (Barr and Spagnolo 2015). To properly include median axis aspect into the classification, its values were transformed into Cartesian coordinates using sine and cosine components (Mardia and Jupp 1999). All variables were standardized into Z scores and checked for collinearities using collinearity diagnostics (minimal variance inflation factors and condition indices). Several clustering methods (between-groups, within-groups, nearest neighbour, furthest neighbour, Ward's) were used for each set of variables (Gareth et al. 2013). A method was discarded if its dendrogram contained classes with only 1–3 cases at the first or second possible cut-off point, otherwise a range of 3–6 potential solutions was derived from the dendrogram and used to generate cluster membership for that clustering method.

Table 1: Calculated morphometric variables.

Morphometric variable	Method of calculation	Reference
Minimum floor altitude	Minimum of altitude values for all cirque pixels	Spagnolo et al. (2017)
Length (L) [a]	The length of the cirque median axis	Spagnolo et al. (2017)
Width (W)	The length of the line perpendicular to the median axis at its midpoint	Spagnolo et al. (2017)
Height (H)	Difference between maximum and minimum altitude	Spagnolo et al. (2017)
L/W ratio	Ratio between length and width	Barr and Spagnolo (2015)
L/H ratio	Ratio between length and height	Barr and Spagnolo (2015)
W/H ratio	Ratio between width and height	Barr and Spagnolo (2015)
Cubic size [b]	$\sqrt[3]{LWH}$	Evans (2006a)
Perimeter (O)	ArcGIS function »Perimeter length«	Spagnolo et al. (2017)
Circularity [c]	O/O_c	Aniya and Welch (1981)
Median axis slope [d]	arctan(Amp/L)	Evans and Cox (1995)
Median axis aspect	Bearing of the cirque median axis	Mîndrescu and Evans (2014)
Plan closure [e]	$360° - (\gamma_{max} - \gamma_{min})$	Hughes et al. (2007); Spagnolo et al. (2017)
Profile closure [f]	$\beta_{max} - \beta_{min}$	Hughes et al. (2007)

[a] A line that connects the cirque threshold midpoint with the top of its headwall and separates the cirque into two parts with an equal surface area. [b] Where L is the length, W the width and H the height of the cirque. [c] Where O is the cirque perimeter and Oc is the perimeter of a circle with the same surface area as the cirque. [d] Where Amp is the altitude range of the median axis and L its length. [e] Where γ_{max} and γ_{min} are the maximum and minimum aspect of the cirque headwall measured towards the cirque centroid at the mean cirque altitude. [f] Where β_{max} is the maximum slope of the cirque headwall and β_{min} the minimum slope of the cirque floor.

2.5 Analysis of variance

Each obtained classification was analysed for the statistical significance of the differences between its classes using the analysis of variance (ANOVA). This analysis has four assumptions: the variables used are on an interval or ratio scale, the variances within the groups are equal and the data for individual groups are independent from one another and normally distributed within each category (Rogerson 2001; IBM 2022). Normality of distribution in all groups was tested using the Kolmogorov-Smirnov statistical test while homogeneity of variances between groups was tested using the Levene test (Rogerson 2001; Field 2013).

Variables were not transformed to satisfy the assumptions of this analysis in order to preserve interpretability, but due to its robustness the ANOVA was still used since some of the assumptions can be violated (Field 2013). For variables with a normal distribution and no homogeneity of variances, the ANOVA's F-test was replaced with the more robust Welch F-test and followed up with the Games-Howell post hoc test, which accounts for both uneven category sizes and heterogenous variances (IBM 2022). For variables with non-normal distributions a non-parametric Kruskal-Wallis test was performed instead since ANOVA is sensitive to violations of the normality of distribution assumption in the case of very unequal group sizes (Field 2013). The omnibus tests were followed up by pairwise comparisons: the Games-Howell post hoc test if the Welch F-test was applied and the Dunn post hoc test with Bonferroni correction if the Kruskal-Wallis test was applied.

2.6 Circular statistics

Circular data were analysed using the R package 'circular' (Agostinelli and Lund 2025; R Foundation … 2025). To analyse circular data across classes, mean directions (φ) and mean resultant lengths ($\bar{R}$) were calculated. The mean directions were assessed for statistical significance using the Rayleigh test (Fisher 1993; Mardia and Jupp 1999). To test for differences between mean directions, the Mardia-Watson-Wheeler test was applied first (Batschelet 1981), followed by pairwise comparisons using the Watson's U^2 test (Watson 1962) with Stephens' correction (Stephens 1970) and Holm-Bonferroni correction, to control for familywise error (Holm 1979). Both tests assume continuous circular distributions and a lack of ties between samples (Batschelet 1981).

2.7 Chi-square tests

Two categorical variables were also analysed: the presence of a cirque threshold and lithology. For both, the Pearson Chi-square test was used to determine potential correlations between cirque type membership and the variable values. The main assumptions of the analysis are: the variables used are categorical, all the observations are independent from one another, each unit can belong to only one cell in the contingency table and the expected count of at least 80% of the cells in the contingency table must be equal to or greater than 5 with no single cell having an expected count of less than 1 (Field 2013). If the last assumption was violated, the Fisher exact test was interpreted instead due to its accuracy with small samples (Fisher 1922). To assess the strength of statistically significant correlations Cramer's V was used (Field 2013). Cirque thresholds were identified using the ArcGIS function »Fill« and the 12.5 m × 12.5 m DEM since it is more hydrologically accurate than its 5 m × 5 m counterpart (Surveying and Mapping Authority of the Republic of Slovenia 2016b). Lithological data were obtained from a version of the lithostratigraphic map made by the Geological Survey of Slovenia (2007) and modified by Hrvatin (2016).

3 Results

3.1 Detection of cirques

Using the predetermined slope and closure thresholds and adhering to the known data on glaciation locations, a total of 86 cirques were manually delineated for the purpose of this research. In the Slovenian part of the Julian Alps (Figure 4), two larger groups of cirques can be observed, one on the ridge between the

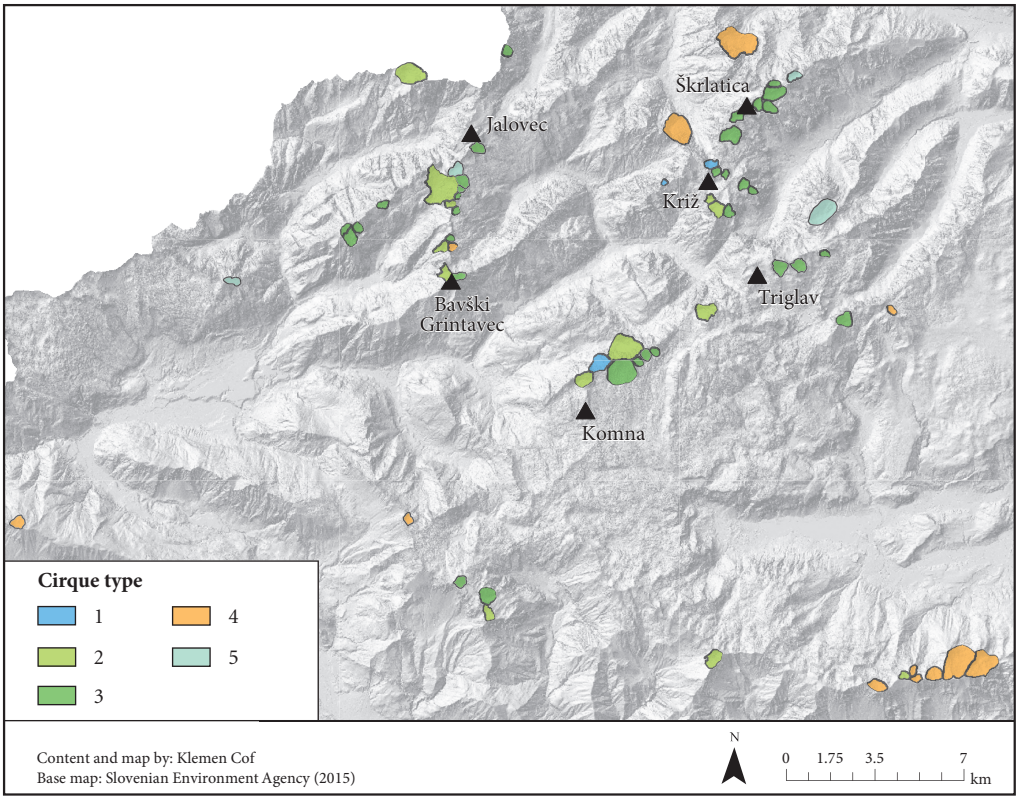

Figure 4: Spatial distribution of cirque types in the Slovenian part of the Julian Alps. See Figure 1 for location in Slovenia.

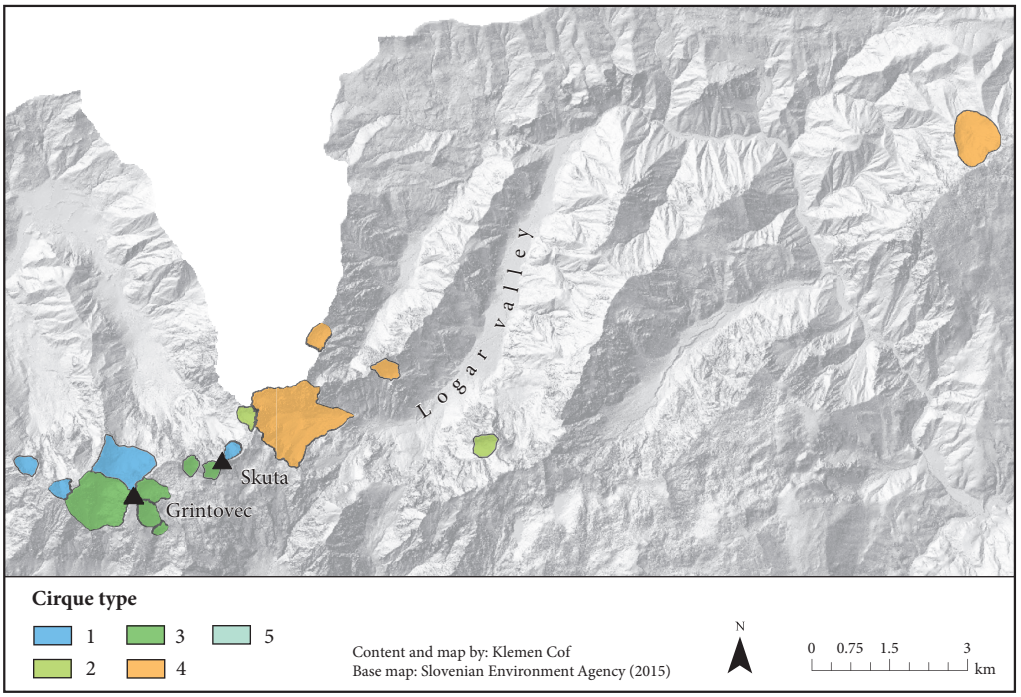

Figure 5: Spatial distribution of cirque types in the Kamnik-Savinja Alps. See Figure 1 for location in Slovenia.

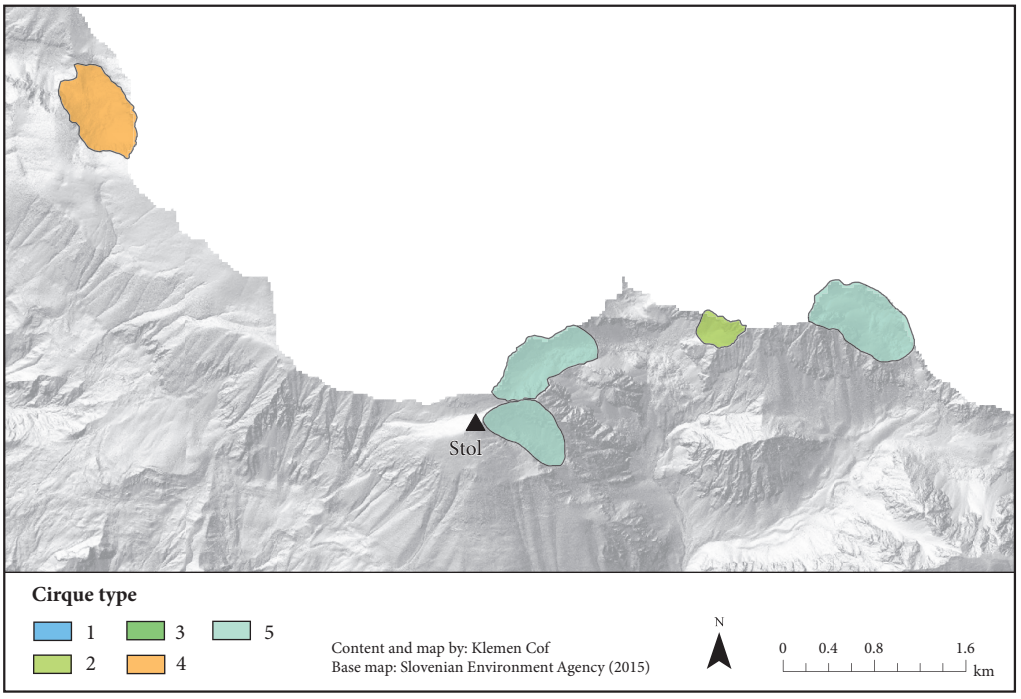

Figure 6: Spatial distribution of cirque types in the Slovenian part of the Karawanks. See Figure 1 for location in Slovenia.

peaks of Mount Bavški Grintavec and Mount Jalovec, and one scattered across the Škrlatica, Križ and Triglav plateaus and the northern fringes of the Komna Plateau. In the Kamnik-Savinja Alps, the cirques are mainly located underneath the peaks of Mount Grintovec and Mount Skuta with a few in the upper reaches of the Logar Valley (Figure 5). In the Slovenian part of the Karawanks, the cirques are located underneath several mountain ridges around Mount Stol (Figure 6). The information about cirque types in Figures 4 through 6 is presented in the subsequent chapter.

3.2 Classification

In the presented classification five cirque variables were used: minimum cirque floor altitude, L/W ratio, median axis slope, the sine and cosine Cartesian coordinates of median axis aspect, and plan closure, resulting in a total of six variables with an insignificant amount of collinearity.

The presented classification was performed using the Ward's Linkage clustering method. From the dendrogram several cut-off points were selected with the one resulting in 5 cirque types yielding the best results. The numbers of cirques in each cirque type across the population and in individual mountain ranges are shown in Table 2. Figures 4 through 6 show the spatial distribution of various cirque types across the Slovenian mountainous regions.

Table 2: Number of cirques of each cirque type in the population and individual mountain ranges, obtained with the presented classification.

Cirque type	Total population	Julian Alps	Kamnik-Savinja Alps	Karawanks
1	7	3	4	0
2	16	13	2	1
3	39	33	6	0
4	17	12	4	1
5	7	4	0	3

3.3 ANOVA

For the presented classification, the means of the following variables were analysed using ANOVA: minimum cirque floor altitude, L/W ratio, L/H ratio, cubic size, circularity, median axis slope, plan closure, and profile closure. Four variables (»Minimum floor altitude,« »L/W ratio,« »Median axis slope« and »Plan closure«) had unequal variances while the other four showed a non-normal distribution between cirque types.

Tables 3 and 4 show the initial results of the two types of ANOVA performed, indicating statistically significant differences at the 0.05 level between cirque types in most variables except for cubic size and profile closure.

Table 5 displays the variable means for all cirque types. A graphical display in the form of box whisker diagrams is shown in Figure 7. The results show that type 4 cirques vary significantly from all other types in terms of minimum floor altitude with mean differences of over 250 m. On average, type 3 cirques have minimum floor altitudes that are over 100 m higher than any other type, though that difference is only significant at the 0.05 level in relation to types 2 and 4. Type 3 also shows the greatest variability in minimum floor altitude. In terms of L/W ratio, type 5 stands out with a significantly higher mean of 1.91 and an interquartile range showing minimal overlap with the other types. Conversely, type 1's mean L/W ratio of 0.78 is significantly lower than all other types, with tight clustering around the mean. The other cirque types' L/W ratios indicate roughly equidimensional planimetric forms. L/H ratios show a similar pattern, where type 1 exhibits a significantly lower and more tightly clustered mean than all other types. Type 5 varies significantly only from types 1 and 3. In terms of cubic size, no cirque type stands out significantly. All cirque types have a roughly equal circularity on average, despite the analysis indicating a significant difference

Table 3: Welch F-test results for the variables »Minimum floor altitude«, »L/W ratio«, »Median axis slope«, and »Plan closure«.

	Statistic[a]	df1	df2	Significance
Minimum floor altitude	21.000	4	21.000	**0.000***
L/W ratio	19.000	4	23.000	**0.000***
Median axis slope	26.000	4	23.000	**0.000***
Plan closure	6.000	4	24.000	**0.001***

[a] Asymptotically F distributed.
* There are statistically significant differences between two or more types at the 0.05 level.

Table 4: Kruskal-Wallis test results for the variables »L/H ratio«, »Cubic size«, »Circularity«, and »Profile closure«.

	Null Hypothesis	Significance	Decision
1	The distribution of L/H ratio is the same across cirque types	**0.000***	Reject the null hypothesis
2	The distribution of Cubic size is the same across cirque types	0.332	Retain the null hypothesis
3	The distribution of Circularity is the same across cirque types	**0.027***	Reject the null hypothesis
4	The distribution of Profile closure is the same across cirque types	0.652	Retain the null hypothesis

Asymptotic significances are displayed.
* There are statistically significant differences between two or more types at the 0.05 level.

Table 5: Variable means for all cirque types for the presented classification.

Variable	Type 1	Type 2	Type 3	Type 4	Type 5
Minimum floor altitude [m a.s.l.]	1903	1794	2033	1519	1900
Length to width (L/W) ratio	0.78	1.21	1.11	1.09	1.91
Length to height (L/H) ratio	0.85	1.55	1.32	1.62	1.98
Cubic size [m]	489	544	440	622	514
Circularity	1.17	1.18	1.12	1.14	1.17
Median axis slope [°]	45.5	27.5	31.4	27.5	22.1
Plan closure [°]	191.6	167.2	166.9	205.7	241.3
Profile closure [°]	66.3	66.3	64.1	66.4	68.0

between types 2 and 3. Consistent with L/H ratios, type 1 cirques have the highest average median axis slopes (45.5°) and differ significantly from all other types. The remaining types have slopes near or below 30°, with type 3 being somewhat steeper (31.4°) and type 5 being the gentlest (22.1°). Despite considerable variability, type 3 still differs significantly from type 5. In terms of plan closure, types 4 and 5 have higher means than types 2 and 3. Type 5 (241.3°) differs significantly from both types 2 and 3 whereas type 4 (205.7°) is only significantly different from type 3 and marginally different ($p = 0.096$) from type 2. Type 1 shows tight clustering around its mean (191.6°) but is not significantly different from the other types. All cirque types have roughly equal average profile closure values. Figure 8 shows a schematic illustration of the five cirque types. Figure 9 shows representative examples for each cirque type.

Figure 7: Box whisker diagrams for all variables, analysed with ANOVA. Circles denote outliers (1.5–3 interquartile ranges from box edge), asterisks denote extreme outliers (>3 interquartile ranges from box edge). ► p. 50

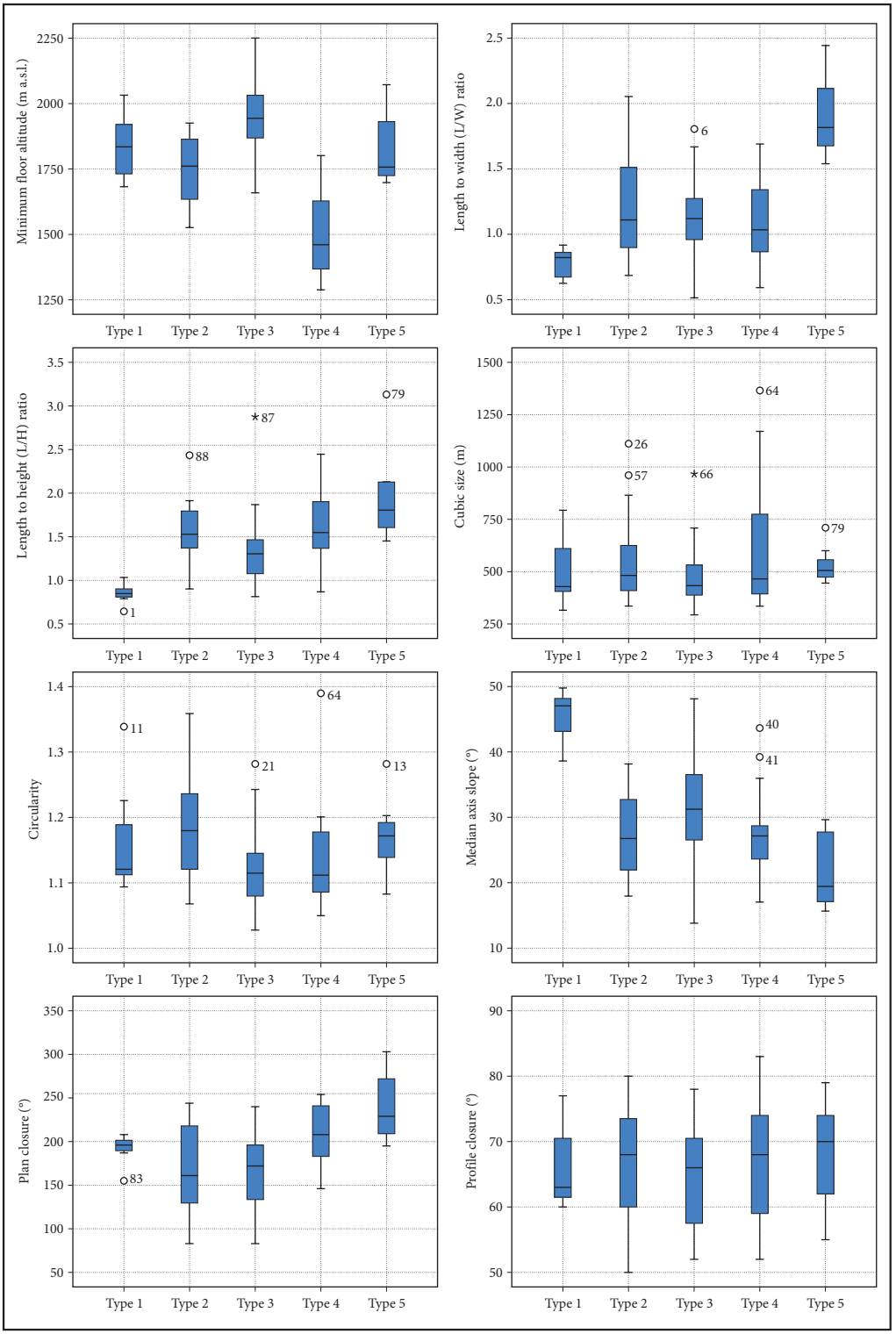
Minimum floor altitude (m a.s.l.)
Length to width (L/W) ratio
Length to height (L/H) ratio
Cubic size (m)
Circularity
Median axis slope (°)
Plan closure (°)
Profile closure (°)
Type 1
Type 2
Type 3
Type 4
Type 5

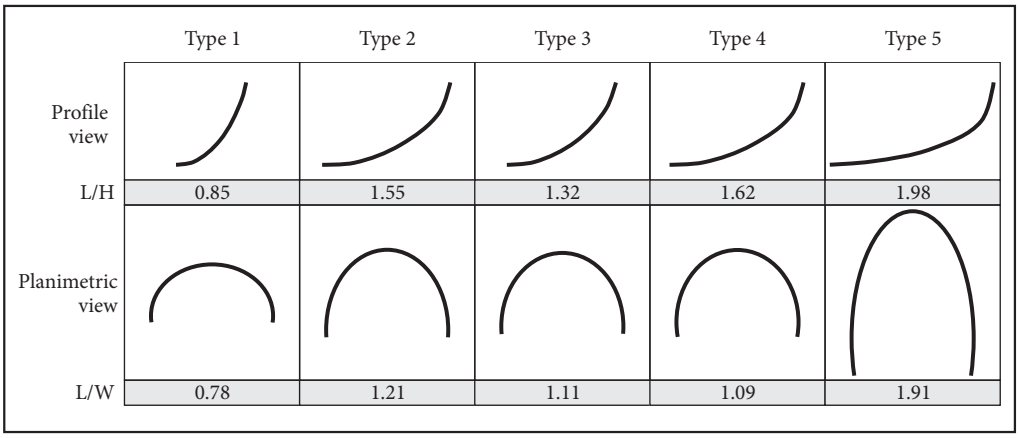

Figure 8: Schematic illustration of the five cirque types in planimetric and profile view.

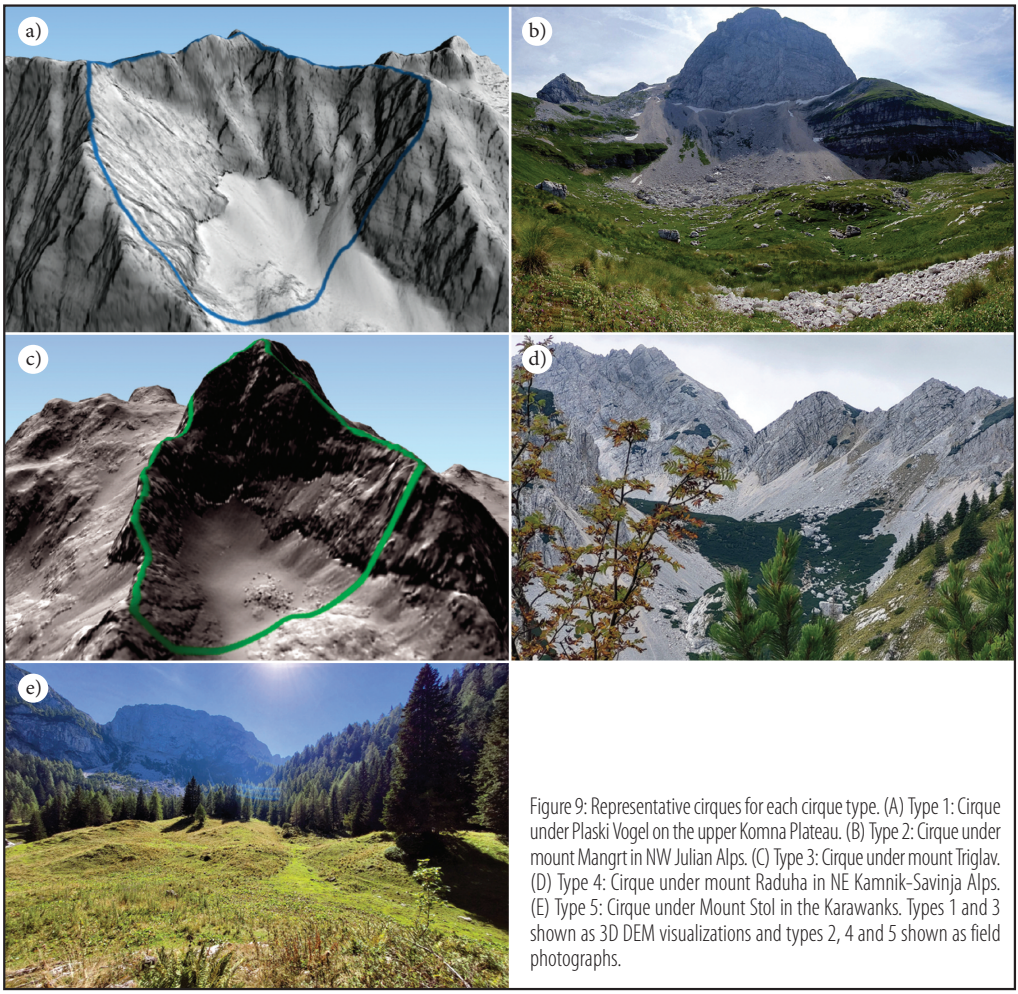

Figure 9: Representative cirques for each cirque type. (A) Type 1: Cirque under Plaski Vogel on the upper Komna Plateau. (B) Type 2: Cirque under mount Mangrt in NW Julian Alps. (C) Type 3: Cirque under mount Triglav. (D) Type 4: Cirque under mount Raduha in NE Kamnik-Savinja Alps. (E) Type 5: Cirque under Mount Stol in the Karawanks. Types 1 and 3 shown as 3D DEM visualizations and types 2, 4 and 5 shown as field photographs.

3.4 Circular statistics

Each cirque type exhibits a very strong concentration around its mean direction, with $\bar{R}$ values of 0.79 or more (Table 6). A graphical display of median axis aspects in the form of percentage-based rose diagrams is shown in Figure 10. All cirque types showed a statistically significant preferred orientation (Rayleigh test: $p < 0.001$ for types 1–4 and $p = 0.005$ for type 5).

Table 6: Circular statistics for median axis aspect for all cirque types for the presented classification.

	Type 1	Type 2	Type 3	Type 4	Type 5
Mean direction [°]	344.7	268.9	136.7	25.8	87.0
Mean resultant length	0.94	0.84	0.82	0.79	0.81

The Mardia-Watson-Wheeler test confirmed the existence of statistically significant differences between the mean directions ($W = 96.61$, $df = 8$, $p < 0.001$) and pairwise comparisons using Watson's U^2 test showed that several of the differences between types are significant. Most notably, type 2 cirques differ significantly from types 3, 4 and 5, and marginally from type 1 as well ($p = 0.050$), facing mainly towards the west. Type 1 cirques are all northward-facing. Their median axis aspects overlap with type 4, but vary significantly (in the case of type 3) or marginally from the other types. Types 3, 4 and 5 all have easterly mean aspect directions, with types 3 and 4 being significantly different from one another.

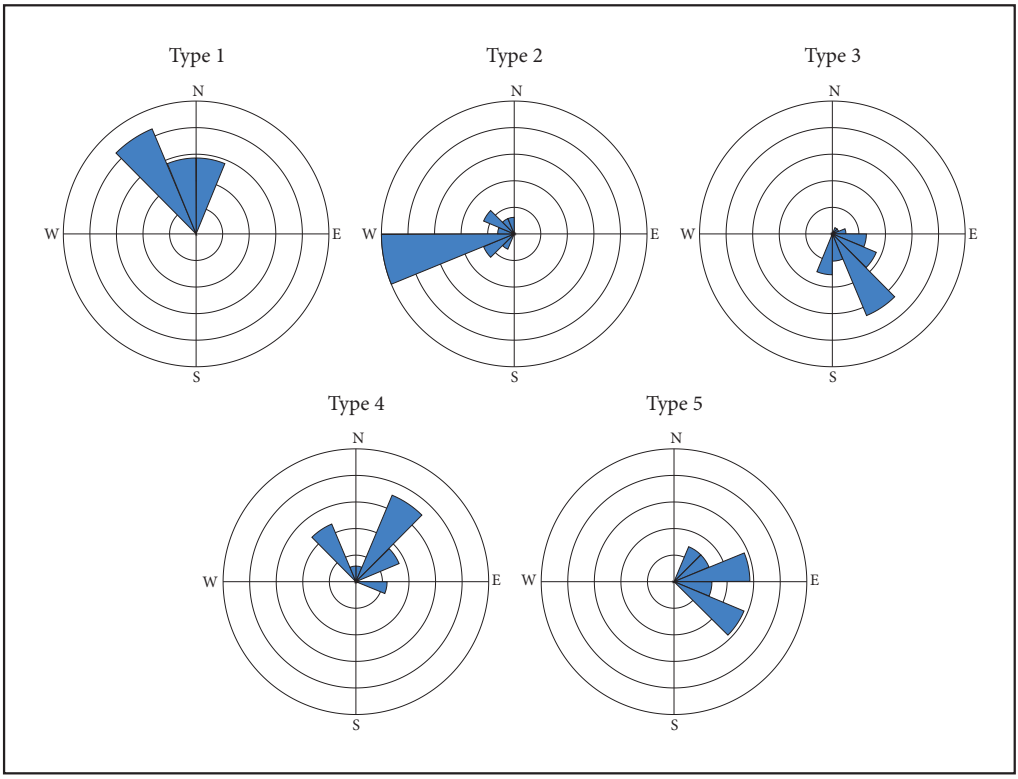

Figure 10: Percentage-based rose diagrams for median axis aspect by cirque type.

3.5 Chi-square tests

A total of 31 cirques contained a well-developed and preserved cirque threshold. While the results of Fisher's exact test (p = 0.286, Cramer's V = 0.248) show no statistically significant association between the presence of cirque thresholds and cirque type membership, some patterns are evident (Figure 11). Types 1 and 4 predominantly (85.7% and 76.5% respectively) contain no preserved cirque threshold while type 5 cirques contain a cirque threshold in 57.1% of cases.

In the case of lithology, Table 7 shows a moderate and statistically significant association between cirque type membership and type of bedrock. It should be noted that the category »Quaternary deposits« encompasses various surface sediments, including talus slope deposits, glacial and alluvial sediments. Similar steps were taken with the various limestone and dolomite bedrocks. Combining lithological categories was necessary to satisfy some of the assumptions of the analysis. As shown in Figure 12, limestones with and without Quaternary deposits appear in all 86 cirques and are the most represented bedrock type. Type 1 cirques occur exclusively in limestones, either with or without overlying Quaternary deposits, and types 2 and 3 show similarly high proportions (75% and 94.9% respectively) of solely limestone-based bedrock. Type 4 displays a much higher proportion (41.2%) of bedrock containing dolomites and clastic rocks. Type 5 cirques are the most predominantly (85%) covered by Quaternary deposits of some kind. Where these Quaternary deposits overlie bedrock, the latter remains the primary factor in cirque formation as the former mostly affect or indicate postglacial modification.

Table 7: Pearson Chi-square, Fisher's exact test, and Cramer's V results for bedrock type in relation to cirque type membership.

	Value	df	Asymptotic significance (2-sided)	Exact significance (2-sided)
Pearson Chi-Square	25.809[a]	16	0.057	
Fisher's Exact Test				**0.017**
Cramer's V	0.274			

[a] 19 cells (76.0%) have expected count less than 5. The minimum expected count is 0.24.

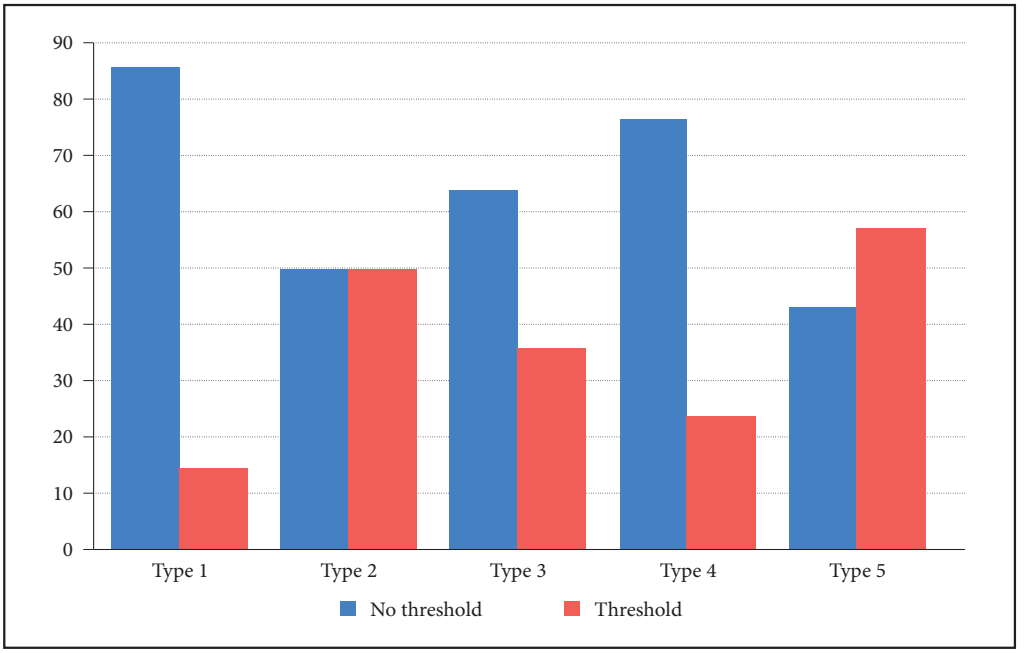

Figure 11: Percentage of cirques with threshold by cirque type.

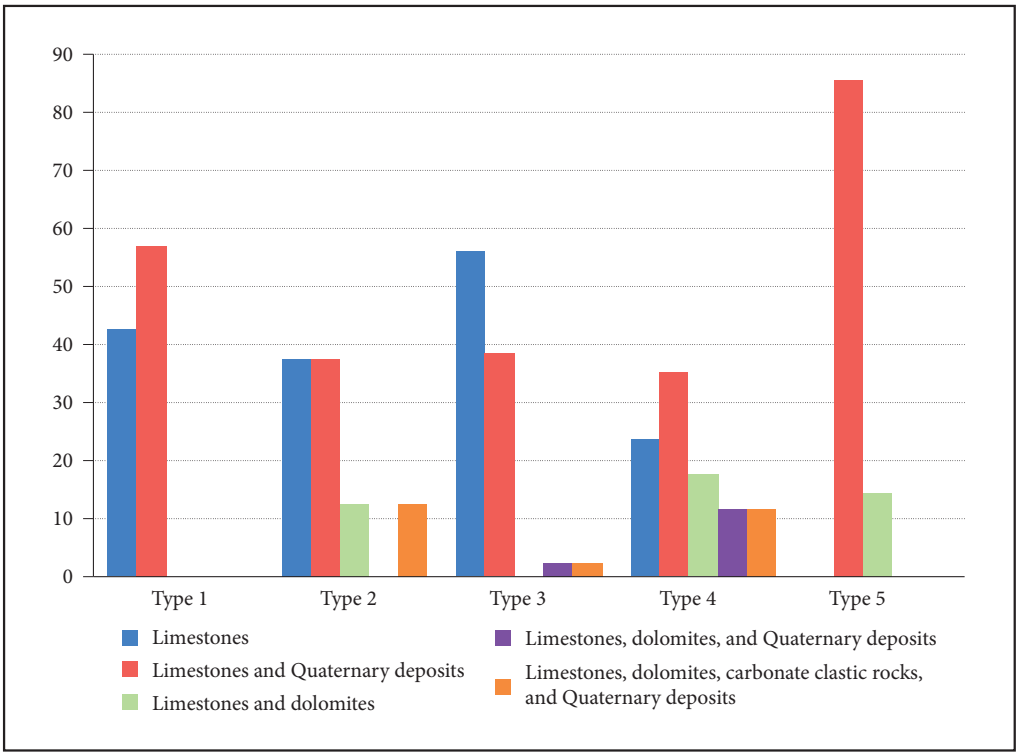

Figure 12: Percentage of bedrock types by cirque type.

4 Discussion

A systematic and objective classification of cirques in Slovenia revealed that among the 86 cirques included in the analysis only 31 exhibit a distinguishable cirque threshold, either due to the high intensity of post-glacial denudation and erosion processes (Bavec and Verbič 2004) or due to intense subglacial erosion in cirques where glaciers flowed beyond their cirques, forming no threshold to begin with. Paired with the lack of dating (Hughes et al. 2021) and research on Slovenian cirques in general this makes the interpretation and assignment of cirques to specific glaciations difficult (Barr and Spagnolo 2015). Based on the results of statistical analyses it is possible to interpret 5 distinct types of cirques in the Slovenian Alps.

Type 1 cirques are located at high altitudes around 1900 m a.s.l. and were formed exclusively in limestones which were later commonly covered by talus slope deposits. They are scattered across the peaks and ridges of the Kamnik-Savinja Alps, where they are most prevalent, along with the northern fringes of the Komna Plateau and the outskirts of the Križ Plateau. They are laterally enlarged and overdeepened, with the highest median axis slopes, which could be partially a result of karst vertical water drainage (Žebre and Stepišnik 2014). This is also likely a factor in their low rate of cirque threshold preservation. Their northward-facing aspects, paired with their relatively high plan closures, indicate reduced exposure to solar radiation (Evans 2006b). These cirques likely contained glaciers bound to their cirques that under favourable conditions effectively overdeepened their cirques rather than extending them (Evans 2006a). They were glaciated for extended periods of time owing to their sheltered high-altitude locations. Their identifying characteristics are their steep profiles and high median axis slopes, as well as their northward aspects, in which they are only similar to type 4.

Type 2 cirques are located at high altitudes around 1800 m a.s.l. and were formed predominantly in limestones. They are found almost exclusively in the Julian Alps on west-facing slopes, with notable con-

centrations around the Komna Plateau, the Križ Plateau and the ridge between the peaks of Mount Bavški Grintavec and Mount Jalovec. They are roughly circular in planimetric form, with lower plan closures. Coupled with higher L/H ratios, this indicates a greater exposure to solar radiation (Evans 2006a). Their predominantly west-facing aspects partially compensated for these unfavourable conditions, allowing these cirques to form on the lower reaches of the LGM glacial extent (Barr et al. 2017). Their westward aspects are their only identifying characteristic as they otherwise share many characteristics with type 3.

Type 3 cirques are located at the highest altitudes, with average floor altitudes around 2000 m a.s.l. They are formed predominantly in limestones with little occurrence of dolomites or clastic rocks. They are the most numerous cirque type, located around Mount Grintovec in the Kamnik-Savinja Alps, as well as in the Julian Alps on the Komna Plateau, the high-altitude plateaus, and the ridge between the peaks of Mount Bavški Grintavec and Mount Jalovec. They have a roughly circular form with lower plan closures and moderate median axis slopes. Their southeast-facing aspects exposed them to increased solar radiation, which is why they were likely formed by small glaciers at the highest altitudes, which enabled cirque growth despite higher ablation rates (Evans 2006b; Barr et al. 2017). Due to their large number and consequently higher variability, they lack a distinguishing characteristic and can only be differentiated from other types based on a combination of characteristics.

Type 4 cirques are located at the lowest altitudes around 1500 m a.s.l., which coincides with the highest occurrence of non-limestone bedrock. Like type 1 cirques, they were commonly covered by talus slope deposits. They are found in all mountain ranges with a notable concentration on the southeastern flanks of the Bohinj basin. These cirques are roughly circular with high plan closures and relatively shallow profiles. Their aspects are the most favourable, being mostly northeast and north-facing, which indicates that solar radiation was a key factor in their formation. These cirques received the least amount of insolation as their headwalls offered additional protection from the Sun during the afternoon, when the surface was somewhat warmer (Evans 1977; Evans 2006a; Barr and Spagnolo 2015). Given their location on the lower fringes of the LGM glacial extent and their morphology, these cirques were likely formed by small glaciers in areas where their favourably facing arcuate headwalls could shelter them from increased ablation brought on by lower altitudes (Evans 1977; Barr et al. 2017). The low degree of cirque threshold preservation was likely caused by a higher intensity of postglacial erosion. Their identifying characteristics are their low elevations along with high plan closures.

Similar to type 1, type 5 cirques are located at high altitudes around 1900 m a.s.l., but with a vastly different morphology. They are mainly found in the Karawanks with some in the Julian Alps. They have eastward aspects and formed in limestones and occasionally dolomites, but were later extensively covered by talus slope deposits along their lengths, indicating a higher rate of postglacial denudation and glaciogenic form and sediment erosion and redeposition (Bavec and Verbič 2004). They are the only cirque type with an elongated planimetric form, with lengths almost double their widths, and consequently they also have the highest plan closures. They are extremely shallow with the gentlest median axis slopes, indicating less glacial overdeepening (Evans 2006a), which is usually caused by glaciers that extended beyond their cirques due to very favourable conditions and lower ELAs. The increased ice accumulation during the LGM allowed these glaciers to extend down valleys despite increased karst drainage (Žebre and Stepišnik 2014; Dixon et al. 2016), with most of the cirque growth occurring during the beginning and ending stages of glaciations (Barr and Spagnolo 2015). In many cases, these cirques retained a cirque threshold, likely a result of gradual glacier retreat and hummocky moraine deposition. Their identifying characteristics are their high L/W and L/H ratios, along with high plan closures and eastward aspects.

It is also possible to infer some of the broader glaciation conditions based on the morphology of cirque types. Varied L/H ratios ranging from 0.85 to 1.98 suggests varied conditions across the three mountain ranges (Ferk et al. 2017). The Kamnik-Savinja Alps contain primarily higher altitude cirque types (75% being types 1, 2 and 3). Given their morphology, it is likely that the ELAs in this mountain range were higher (at 1900 m or above) and that the glaciation conditions were not favourable enough to allow glaciers to extend beyond their cirques, resulting in an absence of type 5 cirques. Instead, some ridges experienced substantial cirque development and overdeepening while others experienced shallower cirque growth. However, varied cirque aspects for these three types (NNW, W, SE) indicate that solar radiation was not a key factor, possibly due to increased cloud cover or wind accumulation (Barr and Spagnolo 2015). The presence of predominantly northeast-facing type 4 cirques on the fringes of the mountain range and the morphological differences between the higher altitude cirques indicate that other strong local topographic

or climatic factors were crucial for cirque formation. These factors caused local differences in subglacial erosion rates, resulting in varied cirque forms, and compensated for higher ablation rates at lower altitudes.

Half of the cirques in the Julian Alps are type 3 with southeast-facing aspects. There is also a considerable number of type 2 cirques, of which the majority are in this mountain range. The presence of cirques on contrasting aspects (west-facing type 2 and eastward-facing types 3 and 5) along many ridges and plateaus indicates favourable glaciation conditions, which is further confirmed by a significant number of type 4 cirques in the region. Judging by the shallow profiles and high plan closures of these low-altitude cirques, the ELAs in the Julian Alps were likely somewhat above 1600–1650 m as altitudes lower than that would be reflected in higher rates of subglacial erosion and a higher representation of overdeepened cirques at lower elevations (Mitchell and Montgomery 2006). The comparatively low frequency of elongated type 5 cirques despite lower ELAs may be a consequence of increased karst drainage (Žebre and Stepišnik 2014) or other topographic factors.

The Slovenian part of the Karawanks has comparatively few cirques, but the prevalence of type 5 cirques indicates very favourable glaciation conditions and ELAs significantly lower than 1900 m, which allowed the glaciers to create elongated cirques that transition into glacial valleys despite the increased karst drainage (Žebre and Stepišnik 2014). At the same time, the glacial ice in the cirques remained mostly frozen to the bed, resulting in reduced subglacial erosion and shallower cirques. Their aspects, however, are likely a consequence of the overall direction of the mountain range and the fact that the Austrian side of the mountain range with cirques potentially facing different directions was not included in the research. Therefore, the aspects of these cirques do not necessarily reflect any past climate conditions and are of limited interpretative use.

The obtained classification is objective, statistically supported, founded on quantitative data, and produced distinct classes. Emphasizing cirque morphometry, this approach provides a rapid and consistent method of partitioning cirques in Slovenia without excessively relying on a researcher's expertise and subjectivity or detailed analyses of each individual cirque. It allows for the subsequent classification of newly discovered cirques in Slovenia, but could be adapted to other cirque populations in the world using the same morphometric variables and accounting for different mountain altitude ranges. Furthermore, this classification offers a preliminary insight into the palaeoclimate properties of Slovenia's mountainous regions and is a foundation for more focused and efficient field studies into the morphometrically varied cirque types and helps determine which methods would likely be useful in their analysis.

5 Conclusion

Cirques, including their morphology and morphometry, are important to inferring palaeoclimate conditions, and an objective classification founded on quantitative data is crucial, especially for regions where cirque populations have yet to be systematically studied. The presented classification was performed using a hierarchical cluster analysis and verified using ANOVA, the Kruskal-Wallis, Watson's U^2 and Chi-square tests. 86 cirques were analysed and classified into five cirque types which can further be split into two subgroups based on altitude; low-altitude (type 4; 1500–1800 m) and high-altitude cirques (types 1, 2, 3 and 5; 1800–2000 m). Based on the prevailing cirque types it is possible to partially infer glaciation conditions in the Slovenian mountains. The Kamnik-Savinja Alps experienced higher altitude glaciation (75% of cirques at 1800–2000 m) with varied rates of subglacial erosion, resulting in both overdeepened and shallower cirques forming on varied aspects (NNW, W, SE) because of increased cloud cover or wind accumulation. The Julian Alps experienced more favourable glaciation conditions which led to more frequent cirque growth on favourable northeastern aspects in low-altitude fringe areas (1500–1650 m) while also enabling more extensive cirque formation on western and eastern aspects at higher altitudes (1800 m and above), with 50% of all cirques in this mountain range facing towards the southeast. The Karawanks experienced favourable glaciation conditions resulting in predominantly east-facing elongated cirques, where glaciers extended beyond the cirques and down valleys. This classification presents a fast and consistent method of classifying new cirque populations and offers an initial exploration into Slovenia's cirque population, establishing a foundation for more detailed future investigations into the factors affecting the formation and modification of the five cirque types.

ACKNOWLEDGEMENTS: The research was partially supported by the Slovenian Research and Innovation Agency Research Programme P6–0101 and the Slovenian Research and Innovation Agency Research Project J6–3141.

RESEARCH DATA: For information on the availability of research data related to the study, please visit the article webpage: https://doi.org/10.3986/AGS.14012.

6 References

Agostinelli, C., Lund, U. 2025: R package 'circular': Circular Statistics (version 0.5–2). *R package*. CRAN. https://doi.org/10.32614/CRAN.package.circular

Aniya, M., Welch, R. 1981: Morphometric analyses of antarctic cirques from photogrammetric measurements. *Geografiska Annaler. Series A, Physical Geography* 63–1,2. https://doi.org/10.2307/520563

Ardelean, F., Drăguț, L., Urdea, P., Török-Oance, M. 2013: Variations in landform definition: a quantitative assessment of differences between five maps of glacial cirques in the Țarcu Mountains (Southern Carpathians, Romania). *Area* 45–3.

Barr, I. D., Ely, J. C., Spagnolo, M., Clark, C. D., Evans, I. S., Pellicer, X. M., Pellitero, R. et al. 2017: Climate patterns during former periods of mountain glaciation in Britain and Ireland: Inferences from the cirque record. *Palaeogeography, Palaeoclimatology, Palaeoecology* 485. https://doi.org/10.1016/j.palaeo.2017.07.001

Barr, I. D., Spagnolo, M. 2013: Palaeoglacial and palaeoclimatic conditions in the NW Pacific, as revealed by a morphometric analysis of cirques upon the Kamchatka Peninsula. *Geomorphology* 192. https://doi.org/10.1016/j.geomorph.2013.03.011

Barr, I. D., Spagnolo, M. 2015: Glacial cirques as palaeoenvironmental indicators: Their potential and limitations. *Earth-Science Reviews* 151. https://doi.org/10.1016/j.earscirev.2015.10.004

Batschelet, E. 1981: Circular statistics in biology. Academic Press.

Bavec, M. 2001: Kvartarni sedimenti Zgornjega Posočja. *Ph.D. thesis*. Univerza v Ljubljani.

Bavec, M., Verbič, T. 2004: The extent of Quaternary glaciations in Slovenia. *Developments in Quaternary Science* 2–1. https://doi.org/10.1016/S1571–0866(04)80088–5

Carr, S. J., Coleman, C. G. 2007: An improved technique for the reconstruction of former glacier mass-balance and dynamics. *Geomorphology* 92–1,2. https://doi.org/10.1016/j.geomorph.2007.02.008

Coleman, C. G., Carr, S. J., Parker, A. G. 2009: Modelling topoclimatic controls on palaeoglaciers: implications for inferring palaeoclimate from geomorphic evidence. *Quaternary Science Reviews* 28–3,4. https://doi.org/10.1016/j.quascirev.2008.10.016

Dixon, J. L., von Blanckenburg, F., Stüwe, K., Christl, M. 2016: Glaciation's topographic control on Holocene erosion at the eastern edge of the Alps. *Earth Surface Dynamics* 4–4. https://doi.org/10.5194/esurf–4–895–2016

Ehlers, J., Gibbard, P. L., Hughes, P. D. (eds.) 2011: Quaternary glaciations – extent and chronology: A closer look. *Developments in Quaternary Sciences* 15. Elsevier.

Evans, I. S. 1977: World-wide variations in the direction and concentration of cirque and glacier aspects. *Geografiska Annaler. Series A, Physical Geography* 59–3,4. https://doi.org/10.2307/520797

Evans, I. S. 1997: Process and form in the erosion of glaciated mountains. In: Process and form in geomorphology. Routledge.

Evans, I. S. 2006a: Allometric development of glacial cirque form: Geological, relief and regional effects on the cirques of Wales. *Geomorphology* 80–3,4. https://doi.org/10.1016/j.geomorph.2006.02.013

Evans, I. S. 2006b: Local aspect asymmetry of mountain glaciation: A global survey of consistency of favoured directions for glacier numbers and altitudes. *Geomorphology* 73–1,2. https://doi.org/10.1016/j.geomorph.2005.07.009

Evans, I. S., Cox, N. J. 1974: Geomorphometry and the operational definition of cirques. *Area* 6–2.

Evans, I. S., Cox, N. J. 1995: The form of glacial cirques in the English Lake District, Cumbria. *Zeitschrift fur Geomorphologie* 39–2.

Evans, I. S., McClean, C. J. 1995: The land surface is not unifractal: variograms, cirque scale and allometry. *Zeitschrift fur Geomorphologie* 101.

Ferk, M., Gabrovec, M., Komac, B., Zorn, M., Stepišnik, U. 2017: Pleistocene glaciation in Mediterranean Slovenia. In: Quaternary glaciation in the Mediterranean mountains. *Special Publications* 433. Geological Society. https://doi.org/10.1144/SP433.2

Field, A. P. 2013: Discovering statistics using IBM SPSS statistics: and sex and drugs and rock 'n' roll. SAGE.

Fisher, N. I. 1993: Statistical analysis of circular data. Cambridge University Press. https://doi.org/10.1017/CBO9780511564345

Fisher, R. A. 1922: On the interpretation of χ^2 from contingency tables, and the calculation of p. *Journal of the Royal Statistical Society* 85–1. https://doi.org/10.2307/2340521

Gareth, J., Witten, D., Hastie, T., Tibshirani, R. 2013: An introduction to statistical learning : with applications in R. Springer.

Geological Survey of Slovenia 2007: Litostratigrafska karta Slovenije. *1:100,000 map*.

Gutiérrez, F., Gutiérrez, M. 2016: Periglacial landforms. In: Landforms of the Earth: An Illustrated Guide. Springer. https://doi.org/10.1007/978–3–319–26947–4_12

Holm, S. 1979: A simple sequentially rejective multiple test procedure. *Scandinavian Journal of Statistics* 6–2.

Hrvatin, M. 2016: Morfometrične značilnosti površja na različnih kamninah v Sloveniji. *Ph.D. thesis*. Univerza na Primorskem.

Hrvatin, M., Tičar, J., Zorn, M. 2020: Rocks and tectonic structure of Slovenia. In: The Geography of Slovenia: Small But Diverse. *World Regional Geography Book Series*. Springer. https://doi.org/10.1007/978–3–030–14066–3_2

Hughes, P. D., Allard, J. L., Woodward, J. C. 2021: The Balkans: glacial landforms from the Last Glacial Maximum. In: European Glacial Landscapes: Maximum Extent of Glaciations. Elsevier. https://doi.org/10.1016/B978–0–12–823498–3.00058–3

Hughes, P. D., Gibbard, P. L., Woodward, J. C. 2007: Geological controls on Pleistocene glaciation and cirque form in Greece. *Geomorphology* 88–3,4. https://doi.org/10.1016/j.geomorph.2006.11.008

IBM 2021: Hierarchical cluster analysis. *Software documentation*.

IBM 2022: IBM SPSS Statistics Base 29. *Software documentation*.

Knight, J., Harrison, S. 2014: Mountain glacial and paraglacial environments under global climate change: lessons from the past, future directions and policy implications. *Geografiska Annaler: Series A, Physical Geography* 96–3. https://doi.org/10.1111/geoa.12051

Kodelja, B., Žebre, M., Stepišnik, U. 2018: Poledenitev Trnovskega gozda. *E–GeograFF* 6. Založba Univerze v Ljubljani. https://doi.org/10.4312/9789612375614

Komac, B., Pavšek, M., Topole, M. 2020: Climate and weather of Slovenia. In: The Geography of Slovenia: Small But Diverse. *World Regional Geography Book Series*. Springer. https://doi.org/10.1007/978–3–030–14066–3_5

Mardia, K. V., Jupp, P. E. 1999: Directional statistics. Wiley. https://doi.org/10.1002/9780470316979

Mîndrescu, M., Evans, I. S. 2014: Cirque form and development in Romania: Allometry and the buzzsaw hypothesis. *Geomorphology* 208. https://doi.org/10.1016/j.geomorph.2013.11.019

Mitchell, S. G., Montgomery, D. R. 2006: Influence of a glacial buzzsaw on the height and morphology of the Cascade Range in central Washington State, USA. *Quaternary Research* 65–1. https://doi.org/10.1016/j.yqres.2005.08.018

Natek, K. 2007: Periglacial landforms in the Pohorje mountains. *Dela* 27. https://doi.org/10.4312/dela.27.247–263

Ogrin, D., Repe, B., Štaut, L., Svetlin, D., Ogrin, M. 2023: Climate classification of Slovenia based on data from the period 1991–2020. *Dela* 59. https://doi.org/10.4312/dela.59.5–89

Penck, A. 1905: Glacial features in the surface of the Alps. *The Journal of Geology* 13–1.

Perko, D., Ciglič, R., Hrvatin, M. 2021: Landscape macrotypologies and microtypologies of Slovenia. *Acta geographica Slovenica* 61–3. https://doi.org/10.3986/AGS.10384

R Foundation for Statistical Computing, R Core Team 2025: R: A language and environment for statistical computing. Computer software.

Rogerson, P. A. 2001: Statistical methods for geography. SAGE Publications. https://doi.org/10.4135/9781849209953

Singh, V. P., Singh, P., Haritashya, U. K. (eds.) 2011: Encyclopedia of snow, ice and glaciers. *Encyclopedia of Earth Sciences Series*. Springer. https://doi.org/10.1007/978–90–481–2642–2

Slovenian Environment Agency 2015: Lidar. *Dataset*.

Spagnolo, M., Pellitero, R., Barr, I. D., Ely, J. C., Pellicer, X. M., Rea, B. R. 2017: ACME, a GIS tool for automated cirque metric extraction. *Geomorphology* 278. https://doi.org/10.1016/j.geomorph.2016.11.018

Steinemann, O., Ivy–Ochs, S., Grazioli, S., Luetscher, M., Fischer, U., Vockenhuber, C., Synal, H. A. 2020: Quantifying glacial erosion on a limestone bed and the relevance for landscape development in the Alps. *Earth Surface Processes and Landforms* 45–6. https://doi.org/10.1002/esp.4812

Stephens, M. A. 1970: Use of the Kolmogorov–Smirnov, Cramér–Von Mises and related statistics without extensive tables. *Journal of the Royal Statistical Society. Series B (Methodological)* 32–1.

Stojilković, B., Stepišnik, U., Žebre, M. 2013: Pleistocenska poledenitev v Logarski dolini. *Dela* 40. https://doi.org/10.4312/dela.40.25–38

Surveying and Mapping Authority of the Republic of Slovenia 2016a: Digitalni model višin 5 × 5 m (DMV 0050). *Dataset*.

Surveying and Mapping Authority of the Republic of Slovenia 2016b: Digitalni model višin 12,5 × 12,5 m (DMV 0125). *Dataset*.

Vilborg, L. 1984: The cirque forms of Central Sweden. *Geografiska Annaler. Series A, Physical Geography* 66–1,2. https://doi.org/10.2307/520939

Watson, G. S. 1962: Goodness-of-fit tests on a circle. II. *Biometrika* 49–1,2. https://doi.org/10.1093/biomet/49.1–2.57

Zhenhua, C. 2011: Exploring new trends of university libraries by SPSS cluster analysis method – Take Wuhan University of Technology as an example. In: 2011 International Conference on Product Innovation Management (ICPIM 2011). Institute of Electrical and Electronics Engineers (IEEE). https://doi.org/10.1109/ICPIM.2011.5983578

Žebre, M., Stepišnik, U. 2014: Reconstruction of Late Pleistocene glaciers on Mount Lovćen, Montenegro. *Quaternary International* 353. https://doi.org/10.1016/j.quaint.2014.05.006

Žebre, M., Stepišnik, U. 2016: Glaciokarst geomorphology of the Northern Dinaric Alps: Snežnik (Slovenia) and Gorski Kotar (Croatia). *Journal of Maps* 12–5. https://doi.org/10.1080/17445647.2015.1095133

Žebre, M., Stepišnik, U., Kodelja, B. 2013: Sledovi pleistocenske poledenitve na Trnovskem gozdu. *Dela* 39. https://doi.org/10.4312/dela.39.157–170